JOURNAL OF GEOPHYSICAL RESEARCH, VOL. 86, NO. A4, PAGES 2286-2294, APRIL 1, 1981

GENERATION OF WHISTLER-MODE SIDEBANDS IN THE MAGNETOSPHERE

C. G. Park

Radioscience Laboratory, Stanford University, Stanford, California 94305

Abstract. VLF transmitter experiments conducted at Siple, Antarctica (L ≃ 4) show that long (≳1 s) keydown signals injected into the magnetosphere often generate sidebands as a result of nonlinear interactions with energetic particles. The spectral characteristics of observed sidebands are quite varied and complex. The sideband frequency spacing varies from ~2 to 100 Hz, but it bears no simple relationship to the carrier amplitude, in sharp contrast to the predictions of some theories. The sideband amplitude is usually 10 dB or more below the carrier amplitude, but sometimes it can exceed the carrier amplitude and also trigger emissions. Multiple sidebands are often observed, and their frequency separations from the carrier may or may not be harmonically related. Sideband amplitudes may be symmetrical or asymmetrical about the carrier. In the asymmetrical case it is usually the upper sideband that is stronger. Various sideband generation mechanisms are discussed in the light of these new experimental data.

1. Introduction

Nonlinear wave-particle interactions between whistler-mode waves and energetic electrons in the magnetosphere have been a subject of many experimental and theoretical studies (see a recent review by Matsumoto [1979] and references therein). One clear evidence of the nonlinear character of the magnetospheric wave amplification process is the fact that when a monochromatic wave is injected into the magnetosphere, the output wave often contains frequencies different from the transmitted frequency. In 'triggered emissions' the output wave frequency changes rapidly with time, forming risers, fallers, or hooks on frequency-time spectrograms [Helliwell, 1965]. Detailed behavior of these triggered emissions and their generation mechanisms have been discussed in a number of papers, including those by Helliwell [1967], Dysthe [1971], Sudan and Ott [1971], Nunn [1974], Helliwell and Crystal [1973], Stiles and Helliwell [1975], Dowden et al. [1978], and Roux and Pellat [1978]. In another category, one or more quasi-constant frequency components appear close to the carrier frequency, with typical spacings ranging from a few Hertz to a few tens of Hertz. It is the purpose of this report to describe these 'sidebands' generated by monochromatic signals from ground-based transmitters.

Previous observations of whistler-mode sideband instability in the magnetosphere have been made by Bell and Helliwell [1971], Likhter et al. [1971], Park and Chang [1978], Helliwell [1979], and Chang et al. [1980]. Bell and Helliwell [1971] observed regular ~0.5-s amplitude pulsations of keydown transmissions from NAA (located in Cutler, Maine) at 14.7 and 17.8 kHz when they analyzed the signal observed at Eights, Antarctica (75°S, 77°W), using a 300-Hz-wide filter. Likhter et al. [1971] reported on observations of amplitude fluctuations with 0.1 to 0.5-s period on long pulse transmissions from a Russian transmitter. Park and Chang [1978], Helliwell [1979], and Chang et al. [1980] showed examples of sidebands generated by the VLF transmitter at Siple, Antarctica (76°S, 84°W; L ≃ 4) and received at the conjugate station, Roberval, Quebec (48°N, 73°W).

A number of theoretical studies have been made of the whistler-mode sideband instability. In the work of Das [1968] and Brinca [1972] an input wave at a given frequency produces fine structures in the particle distribution function near the resonant velocity such that the resulting distribution function is unstable to wave growth at adjacent frequencies. The mechanism studied by Helliwell and Crystal [1973] and by Newman [1977] involves phasing of the waves radiated by stimulated currents (i.e., phase bunching of energetic electrons) that are distributed along a finite length of the wave-particle interaction region. A feedback process between the input and stimulated waves results in oscillatory output wave amplitude. Nunn [1973, 1974] discussed sidebands that arise from a resonance between the sideband wave field and the oscillation period of the phase-trapped electrons. Nunn [1974] also described amplitude pulsations he obtained from computer simulations of long transmitter pulses interacting nonlinearly with the resonant electrons in an inhomogeneous medium. The pulsations apparently result from alternating regions of trapping and detrapping within the interaction region. In the theory of Karpman et al. [1974] a modulational instability develops as a result of nonlinear wave-particle interactions in an inhomogeneous magnetosphere. This instability tends to break up wave trains into smaller wave packets that would be observed as amplitude modulation with a period of the order of the one-hop whistler-mode bounce time. Lashinsky et al. [1980] suggested that sidebands can be generated by the van der Pol oscillator mechanism.

Raghuram et al. [1977] reported on observations of the 'quiet band' phenomenon which has certain similarities to the sideband phenomenon under discussion here. In the quiet band phenomenon an injected monochromatic signal suppresses background hiss in a narrow band (~100-200 Hz) just below the injected signal frequency. This quiet band is often accompanied by a narrow band of enhanced noise below the quiet band. On frequency-time spectrograms the alternate bands of suppressed and enhanced hiss give the appearance of a sideband. This phenomenon was explained in terms of the scattering of near-resonant particles by the injected monochromatic waves in an inhomogeneous medium [Raghuram et al., 1977; Cornilleau-Wehrlin and Gendrin, 1979]. In con-

Paper number 80A1823.
0148-0227/81/080A-1823$01.00

trast to the particle scattering mechanism in the previous paragraph, the quiet band phenomenon involves slow modification of the particle distribution function averaged over many particle bounce periods. (Observed quiet bands develop and decay with time scales of tens of seconds.)

In the next section we present some observational results showing sidebands generated by VLF transmitter signals. Most of the results come from conjugate experiments using a transmitter at Siple and a receiver at Roberval. This will be followed by a discussion of sideband generation mechanisms in the light of the new experimental results.

2. Observations of Sidebands

Figure 1 shows a relatively simple example of sidebands generated by the Siple transmitter and observed at Roberval. The transmitter format was CW, but the frequency was shifted from 4.03 to 4.02 kHz, as clearly indicated in the middle of the record. The symmetric sidebands are ~20 Hz from the carrier, and their frequencies follow the carrier frequency when the latter is suddenly shifted down by 10 Hz. Note that both the carrier and the sidebands show rapid and irregular amplitude fluctuations. Amplitude measurements with a tunable 5-Hz filter at several closely spaced constant frequencies show that on the average the sideband amplitudes are about 10 dB below the carrier amplitude. Similar sideband structure was observed more or less continuously from ~1200 UT until ~1310 UT, although at times the sidebands became intermittent or undetectable. When the transmitter was first turned on it took about 0.5 s for the signal to grow and produce sidebands.

Figure 2 shows another example of Siple transmitter signals with sidebands. The transmitter format was CW, but the frequency was shifted up by 10 Hz on the minute; these frequency shifts are observed at Roberval after one-hop whistler-mode propagation time. In the top panel the transmitter signal at 4.43 kHz is clearly visible but weak until about 1332:50 UT, when the signal becomes intensified and sidebands appear. From

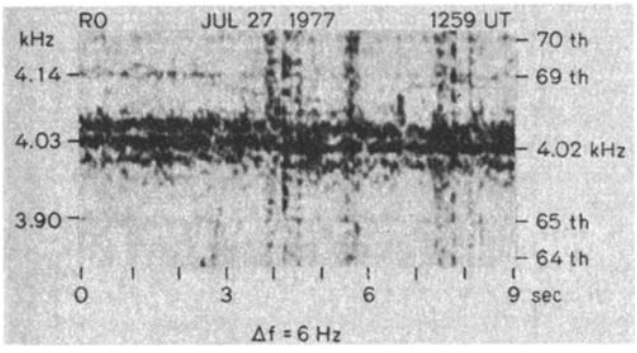

Fig. 1. An example of sidebands generated by the Siple transmitter and observed at Roberval. The keydown transmitter frequency changes from 4.03 to 4.02 kHz at t ≃ 4 s. The harmonic numbers of the local 60-Hz power line frequency at Roberval are indicated on the right [from Park and Chang, 1978].

that time on the sideband structures appear intermittently throughout the rest of the record. The earlier portion of the record shows a fair degree of symmetry about the carrier, with a pair of discrete outermost lines at ±60 Hz and somewhat less well-defined inner structures. The minimum sideband separation discernable on this record is ~10 Hz (see, for example, near t = 10 s in the middle panel). Toward the end of the record the sidebands become broader and less symmetrical, with stronger sidebands appearing on the higher-frequency side.

A portion of Figure 2 near 1333:15 UT is shown in Figure 3 in expanded scales. When the carrier frequency is shifted up by 10 Hz (t ≃ 3 s on the record), the carrier amplitude drops abruptly and the sidebands disappear. The termination of sidebands is marked by an impulse that resembles the 'band-limited impulse' (BLI) discussed by Helliwell [1979]. A BLI is also evident where the frequency shift occurs in the bottom panel of Figure 2. In Figure 3 the carrier amplitude grows with time, and at t ≃ 6 s sidebands reappear with a structure similar to that before the shift in carrier frequency. In particular the outermost pair of sidebands maintain the same spacing of ~60 Hz from the carrier.

Figure 4 shows another portion of Figure 2 in greater detail. (The 6-s segment of Figure 4 is indicated in the middle panel of Figure 2.) The top spectrogram of Figure 4 was made with a frequency resolution of 60 Hz, while the second spectrogram was made with a 6-Hz resolution. As expected, we can see the correspondence between sidebands in the high-frequency resolution record and amplitude fluctuations in the high time resolution record. The two lower panels show amplitude versus time records with filter bandwidths of 300 and 10 Hz, respectively. The 300-Hz filter covers the entire sideband structures, and consequently the output shows amplitude fluctuations corresponding to the sidebands. The bottom panel with a 10-Hz filter bandwidth shows the amplitude of the carrier, excluding the sidebands that are prominent in the second panel. The similar amplitude levels in the two lower panels indicate that most of the signal power is in the carrier rather than in sidebands.

A notable feature in Figure 4 is the lack of any simple relationship between the carrier amplitude and the sideband structure. In particular, the sideband frequency spacing does not appear to depend on the carrier amplitude, a fact which has important implications for the sideband generation mechanism, as discussed in the next section.

To put this in more quantitative terms, sideband separations have been measured at 1-s intervals between 1333 and 1335 UT, and the results are plotted in Figure 5 as a function of wave amplitude. The amplitude measurements were made using a 300-Hz-wide filter, but since the carrier is much stronger than the sidebands, the measured amplitude can be thought of as the carrier amplitude (see Figure 4). It can be seen in Figure 5 that there is no clear relationship between the amplitude and sideband separation.

The top panel of Figure 6 shows an example of strong multiple sidebands on the upper side of the carrier frequency with a regular period of ~0.5 s. The Siple transmitter format was CW at

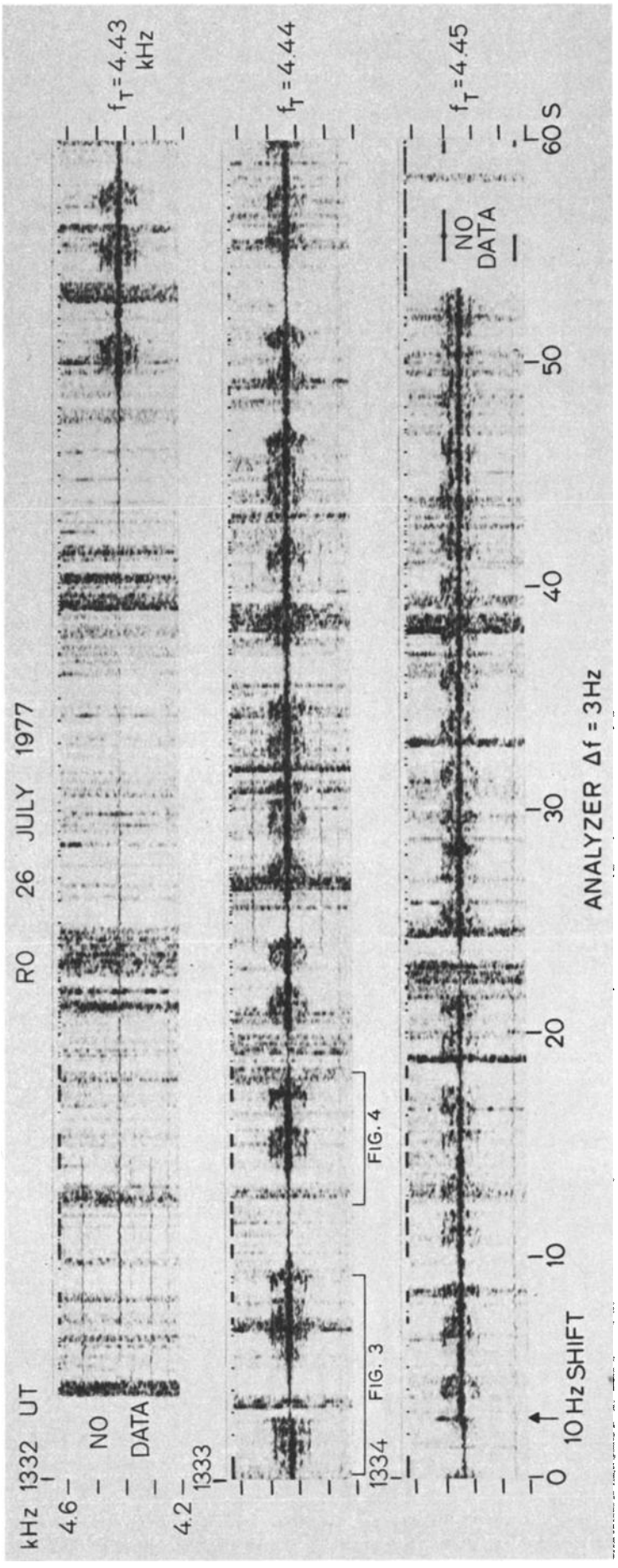

Fig. 2. A 3-min sequence of the Siple transmitter signal and associated sidebands received at Roberval. Parts of the middle panel are reproduced in Figures 3 and 4.

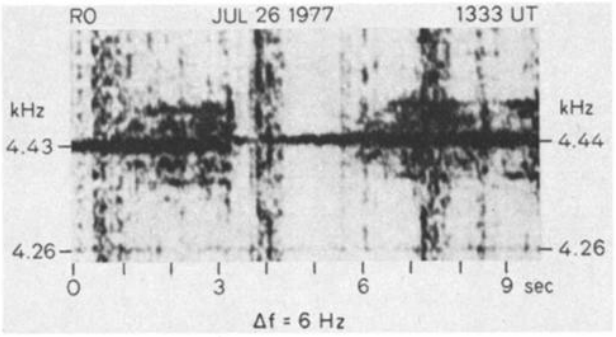

Fig. 3. A portion of Figure 2 reproduced in expanded scales.

4.87 kHz. The lower panels marked A through E display amplitude as a function of frequency at a rate of 20 frequency sweeps per second. The frequency resolution is 6 Hz, the same as the resolution of the dynamic spectrogram at the top of the figure. The analyzer used (Federal Scientific Ubiquitous Model UA-6B/H) employs time compression and data storage techniques that allow the output to be displayed at an arbitrary sweep rate. However, it should be borne in mind that according to the uncertainty principle, the time resoultion $\Delta t \simeq 1/\Delta f \simeq 0.167$ s. This means that the frequency sweeps in Figure 6 do not represent independent measurements unless the frequency sweeps are separated by more than 0.167 s. Each amplitude versus frequency sweep, however, gives a meaningful measurement, although it is not independent of the neighboring sweeps. Note that the sideband amplitude can be comparable to or even exceed the carrier amplitude (see, for example, panel A). Also note that although both the carrier and sidebands have similar amplitude variations with time, their phase relationships are such that strong sidebands are seen when the carrier amplitude is extremely low. A good example of this can be seen in the spectrogram between D and E. It appears that once sidebands are generated they can become independent of the carrier. When the data are analyzed with a 300-Hz filter centered on 4.87 kHz to cover all the sidebands the total amplitude shows a 0.52-s period.

The modulational instability theory [Karpman et al., 1974] predicts amplitude pulsations with periods of the order of the whistler-mode bounce time. In the NAA pulsations reported by Bell and Helliwell [1971] the whistler-mode bounce times were ~0.5 s, close to the amplitude pulsation periods. In the present case, however, the pulsation period in Figure 6 is 0.52 s, whereas the whistler-mode bounce time was found to be 2.15 s at 1501 UT when the keydown transmission started. This is not consistent with the predictions of the modulational instability theory. By comparing the Siple signal bounce time with propagation delays of lightning-induced whistlers it was also found that the Siple signal propagated in a duct located at L = 4.23 with an equatorial electron density of 313 cm^{-3}. Cyclotron resonance with the transmitter signal at the equator would require an electron parallel energy of 640 eV.

Bell and Helliwell [1971] pointed out the possibility that the 0.5-s amplitude pulsation they observed could have been the result of a periodic structure impressed upon the energetic particle population by Pc 1 hydromagnetic waves. To check this possibility for the case in Figure 6, simultaneous ULF recordings from Roberval were analyzed, but no detectable ULF waves were found (A. C. Fraser-Smith, private communication, 1979). The overall sensitivity of the ULF system is conservatively estimated at 1 mγ.

Figure 7 shows the spectrum of a 1-s pulse transmission from Siple observed at Roberval. Near the front of the pulse, temporal growth of the signal is quite evident. At t ≃ 0.85 s, two symmetric sidebands appear at ~±40 Hz from the carrier frequency. At the end of the transmitted pulse a falling tone emission is generated, apparently by the lower sideband. Note that the received pulse is measurably longer than 1 s, indicating multipath propagation. Also note the BLI [Helliwell, 1979] that extends ~150 Hz above the carrier at the end of the pulse. The 1-s pulse transmissions were repeated many times at 10-s intervals, and the same general features illustrated in Figure 7 were observed with each transmitted pulse.

Figure 8 shows two examples of sidebands associated with CW transmissions from NAA (Cutler, Maine; L ~ 3.2) and received at Eights, Antarctica. In the top spectrogram only the upper sideband is seen ~100 Hz above the carrier. The lower panel, taken only 1 min later, shows symmetric sidebands with temporal variations. Between t = 2 and 4 s the sidebands appear with a fairly regular period of about 0.5 s. Second-order sidebands are also evident at ±200 Hz from the carrier.

3. Summary

Sideband observations reported above can be summarized as follows:

1. Although sidebands generally tend to appear when the carrier is strong, there is no simple relationship between the carrier amplitude and sideband frequency separation or sideband amplitude.
2. Sideband separations from the carrier range from ~2 to 100 Hz, but at any given time, sideband separations tend to remain constant even as the sidebands switch on and off. No case has been observed where the sideband separation varies smoothly with the carrier amplitude.
3. Sideband amplitude may be symmetrical or asymmetrical about the carrier. In the asymmetrical case it is usually the upper sideband that is stronger.
4. Multiple sidebands are often observed, and their frequency separations from the carrier may or may not be harmonically related.
5. Sideband amplitude is usually 10 dB or more below the carrier amplitude, but sometimes it can exceed the carrier amplitude and can also trigger emissions.

4. Discussion and Concluding Remarks

Controlled transmitter experiments show that sideband generation is a fairly common phenomenon in the magnetosphere. Since sideband spacing is only a small fraction of the carrier fre-

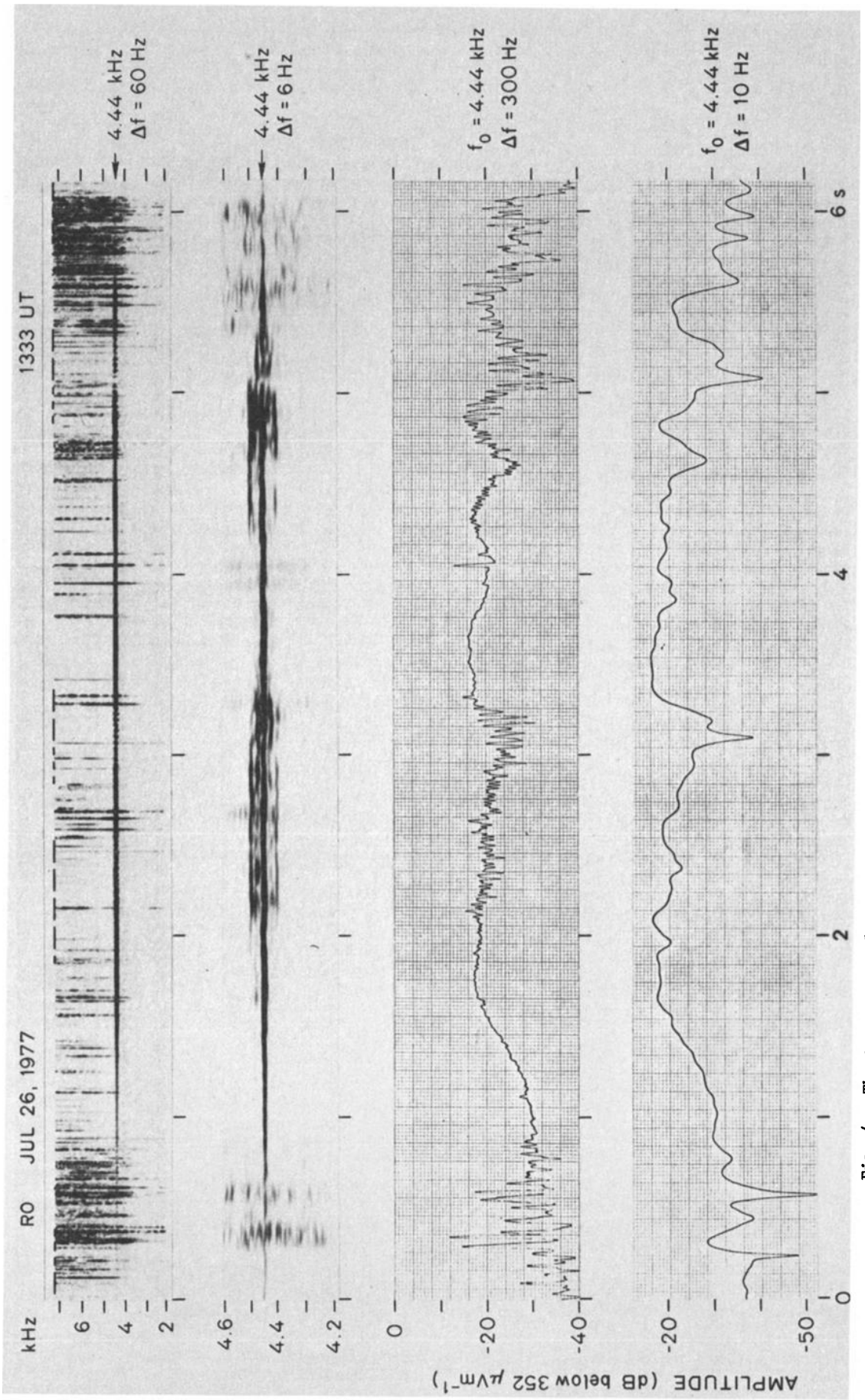

Fig. 4. The top two panels show a portion of Figure 2 in an expanded time scale with two different frequency resolutions of the spectrum analyzer. The two lower panels show the corresponding amplitude variations in two different bandwidths, both centered at the carrier frequency.

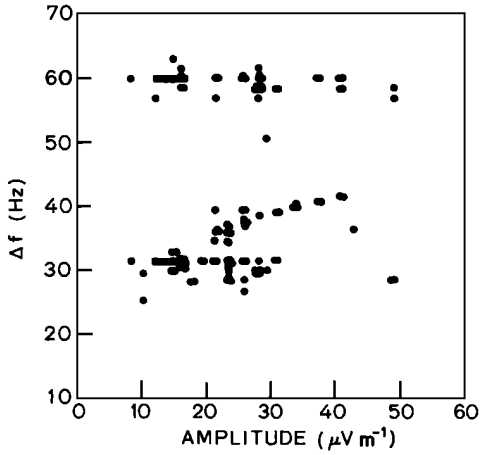

Fig. 5. Sideband frequency separation plotted as a function of wave amplitude for the period 1333-1335 UT, July 26, 1977.

quency (typically ~1%), special high-resolution analysis is needed to identify sidebands. For this reason, no statistical description of the occurrence of sidebands is available at present. However, based on the selected examples illustrated above as well as other studies not included in this paper, it is estimated that perhaps up to 50% or more of magnetospherically amplified transmitter signals lasting more than ~1 s show evidence of sideband structures.

Many theoretical analyses also indicate that sideband generation is an unavoidable consequence of nonlinear wave-particle interactions. Since observed sidebands show a wide variety of spectral characteristics that can very well involve different generation mechanisms, it is difficult at present to rule out any mechanism. However, it is possible to draw a few tentative conclusions regarding some of the proposed mechanisms based on the observations reported here.

In one category of proposed sideband generation mechanisms, the particle phase-trapping frequency plays a key role. The injected wave at one frequency interacts with energetic particles with a finite range of parallel velocities, producing fine structures in the particle distribution functions which are unstable to wave growth at frequencies slightly displaced from the injected wave frequency [Das, 1968; Brinca, 1972]. In an alternative view the sideband wave field resonates with the oscillation of the electrons trapped by the injected wave, thus leading to the growth of sidebands [Nunn, 1974]. According to these theories the frequency separation between the sideband and the carrier is proportional to the particle phase-trapping frequency, which in turn is proportional to the square root of the carrier wave amplitude for a given particle perpendicular velocity $v_\perp$. This presents two difficulties. If there are resonant particles with a range of $v_\perp$, i.e., a range of pitch angles, then we would expect a corresponding spread in the sideband frequency. Thus it is difficult to explain many cases of discrete sidebands illustrated in the previous section. Furthermore, the sideband frequency spacing should vary smoothly with the carrier amplitude; however, this is contrary to what is observed experimentally, as pointed out in the previous section.

Likhter et al. [1971] reported that the sideband frequency spacing showed a dependence on the carrier wave amplitude. This statement, however, was based on a statistical picture and should be interpreted with caution. They stated that the frequency spacing 'varied from [observing] session to session ..., but during the same session it remained approximately constant.' In their statistical picture the observed wave intensity was adjusted for ionospheric absorption according to the local time of the observing session. Thus their limited statistics could have been affected by this normalization procedure. The fact that the sideband spacing remained approximately constant during each session is consistent with our own results reported here.

Another mechanism belonging to the same category of the sideband theories mentioned above was discussed by Abdalla [1970] and Nunn [1974]. In this mechanism, sidebands are generated at the front of a strong injected pulse by the current arising from the motion of particles that suddenly enter the trap of a propagating wave packet. This current lasts only until the trapped particles become completely stirred in the trap. This phenomenon is not observed in our experiments using relatively little power. The observed pulses show temporal growth for about 0.5 s or so before the sidebands become discernible, indicating that the front end of the pulse before temporal growth is too weak to produce the kind of transient effect in question.

A fundamentally different sideband generation mechanism based on a feedback amplification process was discussed by Helliwell and Crystal [1973] and by Newman [1977]. Although there are important differences between the approaches taken by these authors, a common factor is that the sidebands basically result from the phasing between the input wave and the stimulated wave. In this feedback amplifier model the sideband frequency spacing depends on a number of factors but most importantly on the wave propagation and particle transit times across the interaction region. The fact that the sideband spacing does not depend directly on the carrier amplitude is an important advantage of this mechanism over the other mechanisms mentioned above. However, this mechanism runs into difficulties in explaining large sideband spacings of 60 to 100 Hz that are of the same order as the typical trapping period. (Thus far, calculations have been done only for slow pulsations with periods of hundreds of milliseconds.) Another problem is the fact that the observed sidebands are often asymmetric about the carrier, whereas the feedback amplifier mechanism should produce symmetric sidebands. One possible explanation for this apparent discrepancy involves the quiet band phenomenon mentioned in the introduction. Although the quiet band can be observed only when there is background hiss to be suppressed, the same particle scattering process that leads to the quiet band can presumably occur regardless of whether hiss is present. The modified particle distribution function would then suppress the growth of the lower sidebands the same way it suppresses hiss. As pointed out earlier, the quiet band mechanism

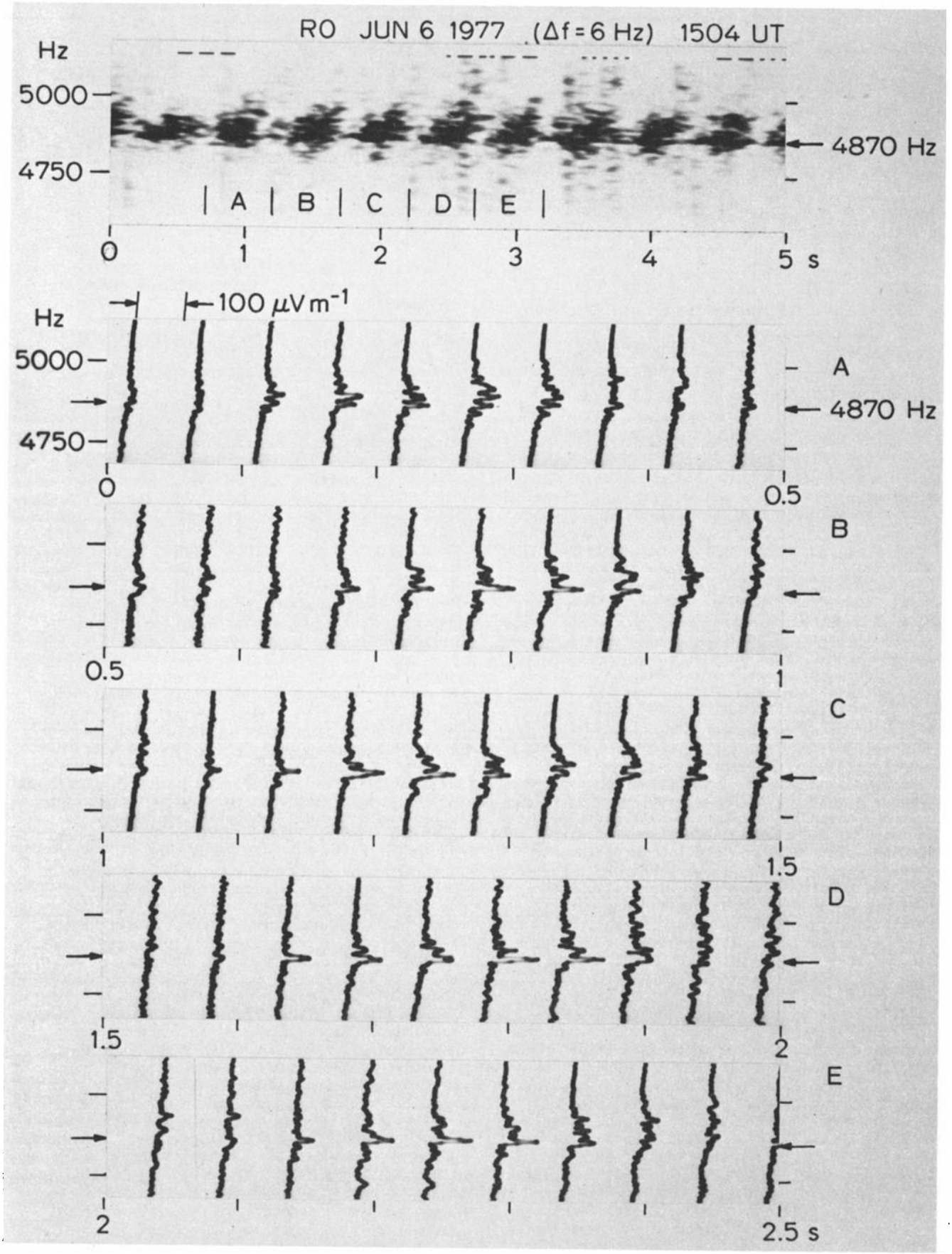

Fig. 6. The top panel shows a dynamic spectrogram from Roberval showing the results of a keydown transmission from Siple at 4870 Hz. Amplitude scans covering portions of the data marked A through E are shown below.

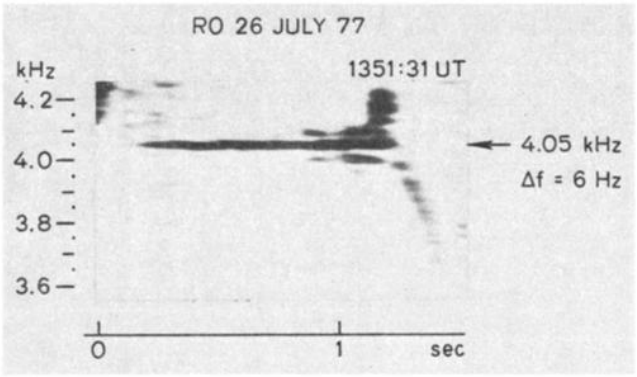

Fig. 7. A 1-s pulse transmission received at Roberval showing sidebands, a falling-tone emission and a band-limited impulse.

involves changes in the particle distribution function over many particle bounce periods and should be distinguished from sideband generation mechanisms discussed by Das [1968], Brinca [1972], and others.

Since the modulational instability theory [Karpman et al., 1971] predicts amplitude pulsations with period of the order of the whistler bounce time, it is not applicable to the observed sidebands with spacings as large as 100 Hz. The van der Pol oscillator mechanism [Lashinsky et al., 1980] involves frequency pulling of natural oscillations by injected waves. This mechanism obviously has difficulty explaining sideband generation in the absence of naturally occurring waves. Nonlinear wave-wave interactions involving hydromagnetic waves or ion cyclotron waves remain a possibility; however, no observational evidence in favor of such a mechanism has been reported to date.

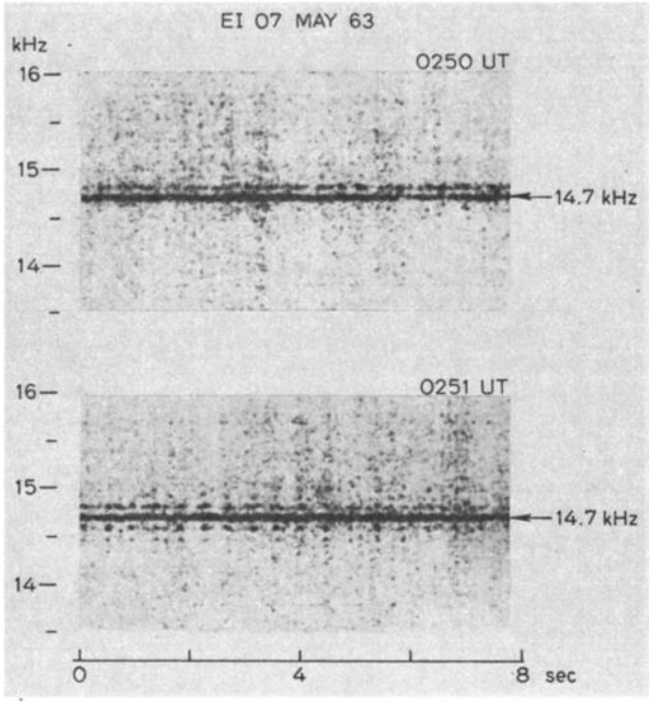

Fig. 8. Two examples of NAA keydown transmissions with associated sideband structures received at Eights, Antarctica.

Acknowledgments. It is a pleasure to acknowledge R. A. Helliwell and D. Nunn for helpful discussions and D. C. D. Chang for his help in data analysis during the early stages of this study. Particular thanks go to J. Yarborough for his exceptional skill and patience in producing the illustrations and to K. Dean for preparation of the typescript. This work was supported in part by the National Science Foundation, Division of Atmospheric Sciences, under grant ATM 78-20967. The data used in this paper were acquired from the experimental programs supported by the National Science Foundation, Division of Polar Programs, under grants DPP76-82646 and DPP78-05746.

The Editor thanks R. Gendrin and D. Nunn for their assistance in evaluating this paper.

References

Abdalla, M., Nonlinear particle trajectories in a whistler mode wave packet, Planet. Space Sci., 18, 1799, 1970.

Bell, T. F., and R. A. Helliwell, Pulsation phenomena observed in long-duration VLF whistler-mode signals, J. Geophys. Res., 76, 8414, 1971.

Brinca, A. L., Whistler sideband growth due to nonlinear wave-particle interaction, J. Geophys. Res., 77, 3508, 1972.

Chang, D. C. D., R. A. Helliwell, and T. F. Bell, Sideband mutual interactions in the magnetosphere, J. Geophys. Res., 85, 1703, 1980.

Cornilleau-Wehrlin, N., and R. Gendrin, VLF transmitter-induced quiet bands: A quantitative interpretation, J. Geophys. Res., 84, 882, 1979.

Das, A. C., A mechanism for VLF emissions, J. Geophys. Res., 73, 7457, 1968.

Dowden, R. L., A. D. McKay, L. E. S. Amon, H. C. Koons, and M. H. Dazey, Linear and nonlinear amplification in the magnetosphere during a 6.6-kHz transmission, J. Geophys. Res., 83, 169, 1978.

Dysthe, K. B., Some studies of triggered whistler emissions, J. Geophys. Res., 76, 6915, 1971.

Helliwell, R. A., Whistlers and related ionospheric phenomena, Stanford University Press, Stanford, Calif., 1965.

Helliwell, R. A., A theory of discrete VLF emissions from the magnetosphere, J. Geophys. Res., 72, 4773, 1967.

Helliwell, R. A., Siple station experiments on wave-particle interactions in the magnetosphere, in Wave Instabilities in Space Plasmas, edited by P. J. Palmadesso and K. Papaddopoulos, p. 191, D. Reidel, Hingham, Mass., 1979.

Helliwell, R. A., and T. L. Crystal, A feedback model of cyclotron interaction between whistler-mode waves and energetic electrons in the magnetosphere, J. Geophys. Res., 78, 7357, 1973.

Karpman, V. I., Ja. N. Istomin, and D. R. Shklyar, Nonlinear frequency shift and self-modulation of the quasi-monochromatic whistlers in the inhomogeneous plasma (magnetosphere), Planet. Space Sci., 22, 859, 1974.

Lashinsky, H. T., T. J. Rosenberg, and D. L. Detrick, Power line radiation: Evidence of van der Pol oscillations, Geophys. Res. Lett., 7, 837, 1980.

Likhter, Ya. I., O. A. Molchanov, and V. M. Chmyrev, Modulation of spectrum and amplitudes of low-frequency signal in the magnetosphere, Sov.

Phys. JETP Engl. Transl., 14, 325, 1971.
Matsumoto, H., Nonlinear whistler-mode interaction and triggered emissions in the magnetosphere: A review, in Wave Instabilities in Space Plasmas, edited by P. J. Palmadesso and K. Papadopoulos, p. 163, D. Reidel, Hingham, Mass., 1979.
Newman, C. E., Theoretical study of amplitude pulsations of 'key-down' whistler-mode signals in the geomagnetosphere, J. Geophys. Res., 82, 105, 1977.
Nunn, D., The sideband instability of electrostatic waves in an inhomogeneous medium, Planet. Space Sci., 21, 67, 1973.
Nunn, D., A self-consistent theory of triggered VLF emissions, Planet. Space Sci., 22, 349, 1974.
Park, C. G., and D. C. D. Chang, Transmitter simulation of power line radiation effects in the magnetosphere, Geophys. Res. Lett., 5, 861, 1978.
Raghuram, R., T. F. Bell, R. A. Helliwell, and J. P. Katsufrakis, Quiet band produced by VLF transmitter signals in the magnetosphere, Geophys. Res. Lett., 4, 199, 1977.
Roux, A., and R. Pellat, A theory of triggered emissions, J. Geophys. Res., 83, 1433, 1978.
Stiles, G. S., and R. A. Helliwell, Frequency-time behavior of artificially stimulated VLF emissions, J. Geophys. Res., 80, 608, 1975.
Sudan, R. N., and E. Ott, Theory of triggered VLF emissions, J. Geophys. Res., 76, 4463, 1971.

(Received July 31, 1980;
revised November 18, 1980;
accepted November 19, 1980.)